Self-Assembly of Janus Nanoparticles in Diblock Copolymers

Li-Tang Yan,[†,*] Nicole Popp,[†] Sujit-Kumar Ghosh,[†] and Alexander Böker[‡,*]

[†]Physikalische Chemie II, Universität Bayreuth, D-95440 Bayreuth, Germany, and [‡]Lehrstuhl für Makromolekulare Materialien und Oberflächen and DWI an der RWTH Aachen e.V., RWTH Aachen University, 52056 Aachen, Germany

ABSTRACT Janus nanoparticles with two chemically different compartments have been shown to be a unique class of building blocks in solution. Here we perform mesoscale simulations to explore the self-assembly of Janus nanoparticles with widely varying architectures in diblock copolymers. We demonstrate that the coassembly of these amphiphilic building blocks forms novel and tunable structures at the interfaces of block copolymers, and consequently influences the interface stabilization and structural evolution kinetics. Our simulations suggest that Janus nanoparticle self-assembly at block copolymer interfaces yields considerable control over the creation of polymer nanocomposites with improved shear behavior. In this context, the approach is a viable strategy for creating functional materials with enhanced processing properties.

KEYWORDS: Janus nanoparticles · diblock copolymers · self-assembly · superstructures · processing properties

Nanoparticles are in the focus of various studies and applications in nanoscience and nanotechnology because of their large variety of novel electronic, optical, biomedical, and magnetic properties.[1−5] In this respect not only the single particles, but especially particle assemblies play an important role. Predicable and precisely ordered superstructures can be constructed if the nanoparticles are "decorated" with specific, anisotropic surface patterns of attractive and repulsive interactions.[6−9] Glotzer *et al.*[10] introduced a "patchy particle" model to study the self-assembly of these new building blocks. Through a unique design with respect to particle size and shape as well as the number and position of the "patches", these particles can successfully self-organize into complex structures in solutions, including chains, sheets, rings, *etc.*[11−13] A unique and emerging type of patchy particles are Janus nanoparticles consisting of two compartments of different chemistry or polarity.[14,15] To date, an impressive number of methods has been developed to fabricate Janus nanoparticles with different geometries in large quantity.[16−21] Since these nanoparticles possess the unique and novel feature of amphiphilicity, they are promising building blocks for directional self-assembly of superstructures that are integral to many of the most useful and complex features of soft materials.[22−25] Also, the Janus character of these nanoparticles provides them with a higher interfacial activity compared to homogeneous particles.[26−30]

A key goal of nanotechnology is the fabrication of complex, highly ordered and functional structures on the nanometer scale.[2−4,10,22−25] The bottom-up self-assembly by combining different building blocks can be an alterative approach to realize this goal. Janus nanoparticles are used as novel building blocks for self-assembly mainly because of their amphiphilicity. Among amphiphiles, prominent examples include not only Janus nanoparticles and other nanoscopic colloids but also molecules like block copolymers.[11] The coassembly of these two different amphiphilic building blocks may lead to novel and complex structures, which can serve as templates for bipolar transport membranes, functional porous media, sensors, *etc.*

On the other hand, the self-assembling block copolymers permit access to various microstructures making them ideal scaffolds for hierarchical control over the size, particle density, and spatial location of the nanoparticles.[31−33] Of particular interest is the control of the assembly of nanoparticles at the interface between different phase domains of the block copolymers.[34,35] Because of their high interfacial activity and amphiphilicity, Janus nanoparticles with chemically different compartments are ideal

*Address correspondence to li-tang.yan@uni-bayreuth.de, boeker@dwi.rwth-aachen.de.

Received for review December 1, 2009 and accepted January 14, 2010.

Published online January 22, 2010. 10.1021/nn901739v

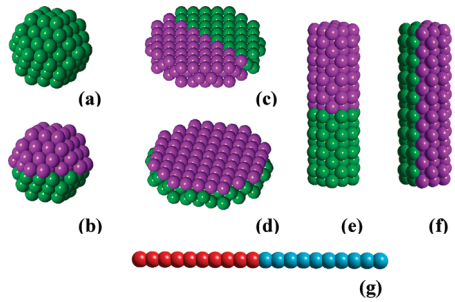

Figure 1. Model building blocks studied in this work. (a) Homogeneous sphere with radius $R_s = 2r_c$ (HS). (b−f) Janus nanoparticles with various architectures. The sites *p* and *q* of every Janus nanoparticle, with an area ratio of about 1:1, are represented by pink and green beads, respectively. (b) Janus sphere with radius $R_s = 2r_c$ (JS). (c) One type of Janus disk with a radius of bottom the face $R_d = 3.5r_c$ and thickness $L_d = 2r_c$ (JD1). (d) The other type of Janus disk with the same size as that of JD1 (JD2). (e) One type of Janus rod with a radius of the bottom face $R_r = 1.5r_c$ and height $L_r = 9r_c$ (JR1). (f) The other type of Janus rod with the same size as that of JR1 (JR2). (g) Symmetric diblock copolymer. Each block consists of 10 beads and blocks A and B are shown by red and blue beads. The red and blue beads in block copolymer have affinities to the pink and green beads in nanoparticles, respectively.

for this purpose. However, the block copolymers do not simply template the ordering of nanoparticles. Rather, the final morphology is determined by a complex interplay between entropy and enthalpy within the system.[36,37] This interplay can be tuned by controlling the size, shape, and coating of nanoparticles. The key in developing new materials is the knowledge on how to exploit this interplay to create the desired structures and expand the repertoire of available morphologies.

We therefore seek to develop an intuitive framework for predicting the self-assembly of a large variety of Janus nanoparticles in diblock copolymers. In this regards, mesoscopic simulations can yield insight into the effects of Janus particle architecture on the kinetic pathway of the self-assembly process and the resulting structures. Our simulations also show that this type of self-assembly can have beneficial effects on the processing properties of the resulting nanocomposites. The simulations demonstrate a viable strategy for creating functional materials with enhanced processing properties.

RESULTS AND DISCUSSIONS

Figure 1 shows the building blocks studied in this work. We address three general classes of Janus nanoparticles including Janus spheres (three-dimensional (3D)), Janus rods (one-dimensional (1D)), and Janus discs (two-dimensional (2D)).[15] The anisotropic rod and disk are divided into two types, respectively, according to their surface designs (Figure 1(c−f)). The area ratio of two sites of the Janus nanoparticles is fixed to about 1:1. Homogeneous nanospheres with a chemically uniform surface were also considered for comparison (Figure 1a). Each nanoparticle is formed from a number of

TABLE 1. The Label and Parameters of Each Type of Nanoparticle Used in the Simulations

label	Figure 1 structure	size (r_c)[a].	beads included	particle number	time steps
HS	a	$R_s = 2$	116	105	3.4×10^5
JS	b	$R_s = 2$	116	105	2.9×10^5
JD1	c	$R_d = 3.5, L_d = 2$	206	59	2.0×10^5
JD2	d	$R_d = 3.5, L_d = 2$	206	59	9.0×10^5
JR1	e	$R_r = 1.5, L_r = 9$	177	69	4.0×10^5
JR2	f	$R_r = 1.5, L_r = 9$	177	69	8.0×10^5

[a] R_s, radius of sphere; R_r, radius of rod bottom face; L_r, height of rod; R_d, radius of disc bottom face; L_d, thickness of disc.

DPD beads arranged on a FCC lattice.[38,39] The bonds between the beads in the nanoparticle are represented by a harmonic spring potential $E_{bond} = K_{bond}((r - b)/r_c)^2$, where $K_{bond} = 64$ and $b = 0.5r_c$ are the bond constant and the equilibrium bond length, respectively.[38] To fairly compare the behavior of spheres with those of rods and discs, these nanoparticles are designed with equal volume fraction and equal net areas based on the relation, $R_s = 3R_{r(d)}v/(2v + 1)$, where R_s is the radius of sphere, R_r and R_d are the radii for the bottom faces of rod and disk, and v is the aspect ratios of rod or disk.[39] The volume fraction of each type of nanoparticle is selected as 0.15 in this work. The symbols and detailed parameters of these nanoparticles are summarized in Table 1. A symmetric diblock copolymer, $A_{10}B_{10}$, is used in the simulations, which self-assembles into a lamellar structure with lamellar thickness about $4.9r_c$. As shown in Figure 1, the red (block A) and blue (block B) beads in the block copolymer have an affinity to the pink (site *q*) and green (site *p*) beads in the nanoparticles, respectively.

The simulations start from randomly dispersed block copolymers and nanoparticles. The simulation time ranges from 2.0×10^5 to 9.0×10^5 time steps depending on the structure evolution which should ensure that the system reaches the equilibrium state (Table 1). Figure 2 shows the equilibrium self-assemblies formed by various nanoparticles in block copolymers. To visualize the 3D structures of these nanocomposites more clearly, we use the image format of isosurface where the interfaces between two phase domains are represented by a series of isosurfaces. Details on the image formats can be seen in Supporting Information, Figure S1. The homogeneous spheres with uniform surface beads are clearly observed to be located near the center of their preferential lamellae (Figure 2a). Essentially, the location of nanoparticles in diblock copolymers can be rationalized on the basis of the interplay between enthalpy and entropy involving A,B blocks and the surface coating of the nanoparticles.[36,37] A significant conformational entropy penalty of polymer chains will be induced if the homogeneous spheres are excluded from the lamella center because of their large size.[37] In contrast to the homogeneous spheres, the Janus spheres

with two compartments of different beads segregate to the interface between two lamellae (Figure 1b). This reveals that the enthalpic effects from the interactions between A,B blocks and the surface of Janus nanoparticles overcome the entropic effects from the conformation transition of polymer chains.

This strong enthalpic effect also anchors the Janus rods and discs at the interface (Figure 1c−f). We can find that these anisotropic Janus nanoparticles self-assemble into regular structures at the interface of block copolymers, except for JD2 (Figure 2f) where large interfacial fluctuations persist even in the equilibrium state. It is interesting that the orientation of these anisotropic Janus nanoparticles with respect to the interface can be controlled upon changing their surface architectures. If the connecting surface between two sites of a Janus nanoparticle is perpendicular to the orientation direction of the particle, for example, JR1 and JD1, its orientation direction in the self-assembly will be perpendicular to the interface, leading to "standing" particle structures (Figure 2c,e). For Janus nanoparticles like JR2 and JD2 where the connecting surface between the two surface sites is parallel to the orientation direction of the particle, its orientation direction in the self-assembly will be parallel to the interface, leading to "lying" particle structures (Figure 2d,f). In the case of anisotropic nanoparticles with homogeneous surface chemistry, their orientation can only be parallel to the polymer lamellae due to the entropic effects from the deforming polymer chains.[33] Thus, the Janus character of anisotropic particles provides additional options to direct their assembly at polymer interfaces.

It should be pointed out that the interaction parameter between the beads of the two sites of the Janus nanoparticles is set to be equal to that between like beads in the simulations because the present work only concerns the relation between nanoparticles and the interface. Thus no preferential interaction takes place between two Janus nanoparticles. However, we anticipate that Janus nanoparticles can self-assemble and pack at the interface if the interaction between two surface sites is preferential and strong enough, resulting in "standing" or "lying" superstructures at the interface. The interfacial structures of block copolymers can also be tuned by applying external fields, for example, electric field,[40] shear field,[41] *etc*. Consequently the particle structures or superstructures at the interface can be oriented on the macroscopic scale within their scaffold, which however is very difficult to realize in solutions.

In addition to the general orientation of the Janus nanoparticles, in Figure 2, we find that almost all "standing" Janus nanoparticles (JR1 and JD1) are absolutely perpendicular to the interface as shown in Figure 2c,e. If the orientation of these Janus nanoparticles was completely dominated by the enthalpic effects, they would have a tilted orientation with respect to the interface as long as the two surface sites are located in their preferential lamellae. Another interesting observation is that only the "lying" Janus discs (JD2) can induce large interfacial fluctuation in the equilibrium state.

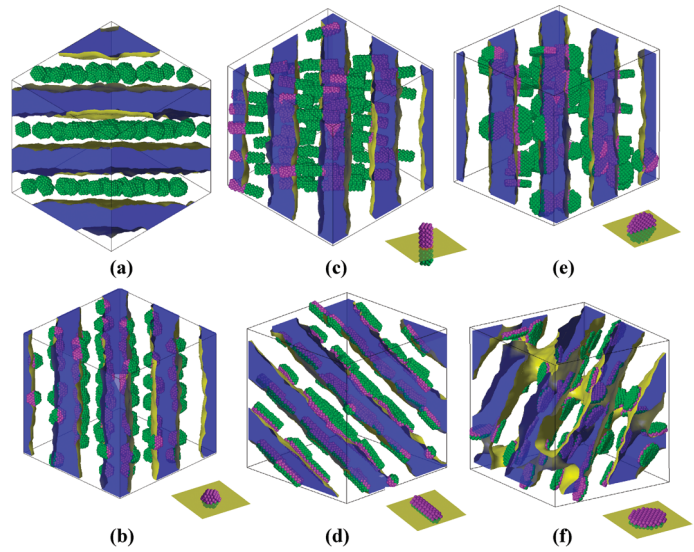

Figure 2. Equilibrium self-assemblies formed by various nanoparticles in symmetric diblock copolymers. The volume fraction of each type of nanoparticle is 0.15. The interface between phases A and B is colored yellow, and phase A is colored half-transparently blue. Phase B is fully transparent. The types of nanoparticles are (a) HS, (b) JS, (c) JR1, (d) JR2, (e) JD1, and (f) JD2. The code of these nanoparticle labels is given in Figure 1 and Table 1. The schematic diagrams at the right bottom of images b−f illustrate the orientation of Janus nanoparticles with respect to the interface.

To understand both observations, we gain insight into the conformations of polymer chains in the vicinity of the Janus nanoparticles. For this purpose, a single Janus nanoparticle with polymer chains around it has been extracted from the equilibrium self-assembly (Figure 3A). A cluster of polymer chains in the local interface of the pure diblock copolymers is also shown in Figure 3b. In the absence of nanoparticles the collapsed polymer chains accumulate and form a uniform interface between two phase domains (Figure 3b). The presence of "standing" Janus nanoparticles (JR1, JD1) as well as Janus sphere (JS) does not influence the chain conformations much (Figure 3a,c,e). In the cases where the Janus nanoparticle orientation is tilted with respect to the normal of the interface, they will deform the polymer chains in their vicinity (see Supporting Information, Figure S2). According to the strong segregation theory based on polymer brushes,[42] the pressure due to the chain deformation acting at a distance l from the interface ($l = 0$) is given by $P(l) \propto h^2(1 - l^2/h^2)$, where h is the height of the brush formed by polymer chains. The entropic energy loss, E_p, is consequently given by $dE_p(l) \approx P(l)\, dV$ where dV is the differential volume of the nanoparticles at distance l. Apparently, the chain deformation would lead to a pressure and thus entropic energy penalty. Therefore we attribute the perpendicular orientation of JR1 and JD1 in the interface to the entropic effects associated with the deformed polymer chains in the vicinity of the Janus particle.[33]

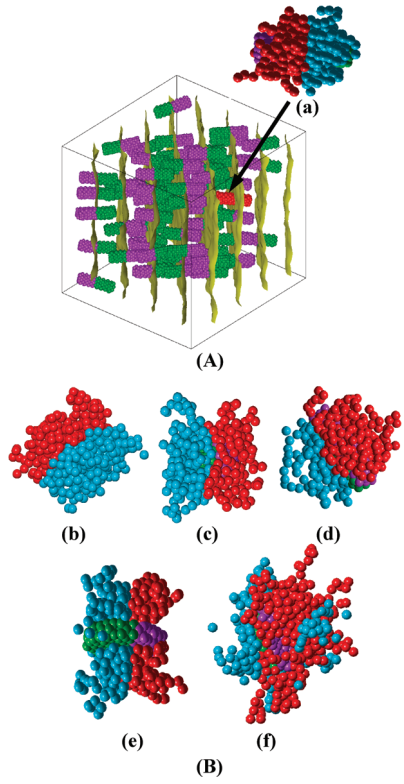

Figure 3. The conformations of polymer chains in the vicinity of Janus nanoparticles. (A) A simulation snapshot of the composite with symmetric diblock copolymer and JR1 particle at 20000τ, representative of a typical co-self-assembly of block copolymer−Janus nanoparticle systems. Here only the interface between the two phases (yellow surfaces) and the Janus rods is shown for clarity. A single Janus rod (marked in red) has been selected from the simulation cell to demonstrate the conformation of polymer chains around it. (B) Typical polymer chain conformation obtained as shown in (A) from the equilibrium systems of symmetric diblock copolymers without or with various types of Janus nanoparticles: (a) JR1, (b) without nanoparticles, (c) JS, (d) JR2, (e) JD1, and (f) JD2. The code of these nanoparticle symbols and beads can be seen in Figure 1 and Table 1.

In contrast to "standing" cases, the "lying" Janus nanoparticles, especially JD2, can significantly influence the conformations of the surrounding polymer chains (Figure 3d,f). Here, the polymer chains have to stretch in order to fill the space around the nanoparticles leading to a larger interfacial fluctuation. The scale of the interfacial fluctuation induced by different Janus nanoparticles can also be rationalized on the calculation of interface tension using the following equation:[43]

$$\frac{-\gamma_{Ap}+\gamma_{Bp}}{\gamma_{AB}}\frac{1}{R_p} \le \frac{1}{R_i} \le \frac{-\gamma_{Aq}+\gamma_{Bq}}{\gamma_{AB}}\frac{1}{R_p} \qquad (1)$$

where γ is the interfacial tension corresponding to the components indicated by the subscript label. R_i is the curvature of the interface near the Janus nanoparticles. R_p is the radius or equivalent radius of the particle section contacting the interface. According to the interaction parameters between different beads used in the present work, γ_{Aq} and γ_{Ap} are equal to γ_{Bp} and γ_{Bq}, respectively.[44] Then it can be seen that $-\gamma_{Ap}+\gamma_{Bp} = -(-\gamma_{Aq}+\gamma_{Bq})$. Thus, eq 1 reveals that the scale of interfacial fluctuation (or the curvature of the interface, R_i) induced by a Janus nanoparticle should be monotonously proportional to R_p. The R_p of JD2 is the largest among all types of nanoparticles considered in this work and consequently produces a larger interfacial fluctuation than all other Janus nanoparticles.

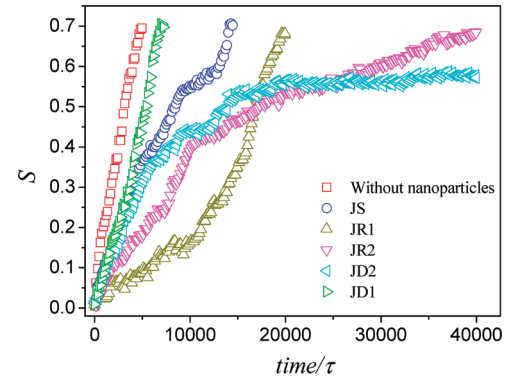

Figure 4. Order parameter (*S*) as function of simulation time for various systems. The symmetric diblock copolymer without or with Janus nanoparticles are compared to show the effect of Janus nanoparticles with different architectures on the structural evolution kinetics of nanocomposites. The code of these nanoparticle symbols can be found in Figure 1 and Table 1. The volume fraction of each type of nanoparticle is 0.15.

In the following we consider how the architecture of a Janus nanoparticle influences the structural evolution kinetics of the nanocomposites containing block copolymer and Janus nanoparticles. To quantify the kinetics of these composites, we calculate the order parameter defined by the Saupe tensor,[45] that is, $Q_{\alpha\beta} = 1.5\hat{\mathbf{r}}_\alpha\hat{\mathbf{r}}_\beta - 0.5\delta_{\alpha\beta}$, where α and β are Cartesian indices, δ is the Kronecker symbol, and $\hat{\mathbf{r}}$ is a unit vector along the chain axis from the center of block *A* to the center of block *B*. The largest eigenvalue of the volume average $Q_{\alpha\beta}$ is the order parameter *S*. *S* is zero for block copolymer in the completely disordered state and unity for the block copolymer in the ordered and aligned state.

In Figure 4 the order parameters are plotted *versus* the evolution time for various systems, revealing the effect of the Janus architecture on the kinetics of these nanocomposites. Clearly, the pure diblock copolymers hold the fastest kinetics, and a longer time is needed for the systems of "lying" Janus nanoparticles (JR2, JD2) to reach the ordered structures than that for the systems of "standing" Janus nanoparticles (JR1, JD1) as well as the Janus sphere. A detailed kinetic pathway of block copolymer−Janus sphere composite can be seen in Supporting Information, Figure S3. It demonstrates that the strong interactions between polymer blocks and sphere surface keep the Janus nanoparticles attaching to the interface during the process. The Janus nanoparticles anchoring in the interface will depress the evolution of nanocomposites and leads to sluggish kinetics in comparison to that of the pure diblock copolymers. As

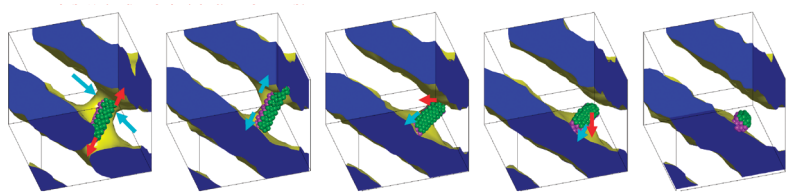

Figure 5. Detailed assembling process of a single Janus rod confined within polymer lamellae. The snapshots are extracted from the block copolymer−JR2 composite (see Figure S5 and the video in the Supporting Information). The side length of the cubic lattice size is $16r_c$. The time of each snapshot is 39275τ (a), 39550τ (b), 39975τ (c), 40000τ (d), and 40025τ (e). The cyan and red arrows indicate the direction of the fluctuations of polymer phase and the rod, respectively. The interface between phases A and B is colored yellow and phase A is colored blue. Phase B is fully transparent.

shown in Figure 3, the "lying" Janus nanoparticles can induce larger fluctuation or defects in the interface than the "standing" Janus nanoparticles. Overcoming these additional defects also requires a longer time. Figure 4 demonstrates that the kinetics of "lying" Janus nanoparticles turns out to be very slow at the later stage. This may be due to the increasing interaction frequency among Janus nanoparticles as they are confined to the interface that forms in the later stage. Moreover, the "lying" Janus nanoparticles have a larger contact area with the interface which consequently decreases the diffusion ability of these nanoparticles. The assumptions have been confirmed by calculating and comparing the mean-square displacement (MSD) of JR1 and JD1 nanoparticles (see supporting Supporting Information, Figure S4).

Another important factor accounting for the retarded kinetics of "lying" Janus nanoparticles is the spatial confinement effect. The sizes of JR2 and JD2 in the longest axes are $9r_c$ and $7r_c$, respectively, which are bigger than the lamellar thickness of block copolymers ($4.9r_c$). Therefore the rotation and translation of these "lying" Janus nanoparticles are facing the spatial confinement from polymer lamellae especially in the later stage. To get more detailed insight into the mechanism of this effect, a small lattice with side length $16r_c$ with a single JR2 nanoparticle has been extracted from the simulation cell to display the assembling process of the "lying" Janus nanoparticle confined within polymer lamellae (see Supporting Information, Figure S5). The details of this process can be seen from the video in the Supporting Information. Figure 5 shows a series of snapshots to demonstrate this process. Here the cyan and red arrows indicate the direction of the fluctuations of the polymer phase and the rod, respectively. Initially the Janus rod attaches to an interconnection between two lamellae. The interconnection fluctuates in the plane parallel to the lamellae while the rod fluctuates up and down along it (Figure 5a). Then a neck zone forms in the interconnection with two sections shrinking toward their supported lamellae. However, the site of the anchored Janus rod limits the shrinkage of its preferential phase. Thus these two sections turn to fluctuate along the particle (Figure 5b). Meanwhile the phase shrinkage gradually dominates this process and one section arrives at its destination providing the space for the rod to rotate and move (Figure 5c). Then the shrinkage of the other interconnection section draws the rod toward the lamella quickly (Figure 5d) and finally the Janus rod lies on the interface (Figure 5e). The process shown in Figure 5 offers a clear view about the interplay between the polymer phase and the Janus nanoparticle in a spatial confinement state which influences the kinetic pathway for structural evolution of these nanocomposites. The thickness of the lamella can be tuned by changing the length of the polymer chains. Therefore we anticipate that the spatial confinement state of the certain Janus nanoparticle can be controlled by selecting diblock copolymers with different chain lengths.

To delineate the practical usefulness of block copolymer−Janus nanoparticle self-assembly, we have investigated the shear behavior of the nanocomposites. The shear field is introduced to these systems by using the Lees−Edwards boundary condition,[46] the details of which can be found in Supporting Information. The shear viscosity is calculated based on the pressure tensor, $P_{\alpha\beta}$, which is measured by

$$P_{\alpha\beta} = \frac{1}{V}\langle \sum_i m_i v_{i,\alpha} v_{i,\beta} \rangle + \frac{1}{V}\langle \sum_i \sum_{j>i} F^{c}_{ij,\alpha} r_{ij,\beta} \rangle \qquad (2)$$

where V is the volume of the simulation box.[47] Shear viscosity in association with the only nonvanishing off-diagonal component, P_{yz}, is given by $\eta = -P_{yz}/\dot{\gamma}$ where η is the non-Newtonian shear viscosity and $\dot{\gamma}$ is the shear rate.[47] The shear field is initially applied to the equilibrium structures with shear rate $\dot{\gamma} = 0.01$ which is not too large and can avoid the potential microturbulence. For comparison, we only consider the shear behavior of pure block copolymers and two nanocomposites of block copolymers with homogeneous and Janus spheres (HS and JS), respectively.

Figure 6 shows the temporal evolution of the order parameter for these three systems. The order parameter curves show an initial drop with some fluctuation and then rise slowly to finally level off. This monitoring of order parameter is clarified by the structure changes of the block copolymer−Janus sphere composite during the shear process (see Supporting Information Fig-

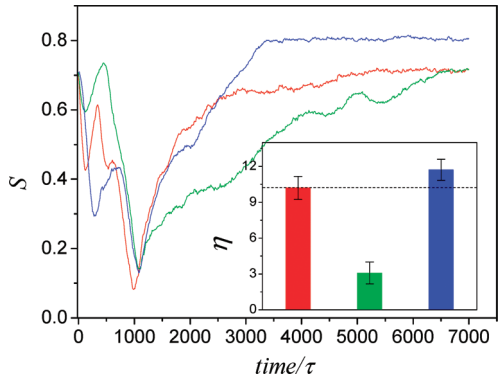

Figure 6. Order parameter (*S*) as functions of shear time. The inset shows the shear viscosity (η) at the later stage: (red) pure block copolymers, (green) block copolymer−HS nanocomposite, and (blue) block copolymer−JS nanocomposite. The code of the nanoparticle symbols can be found in Figure 1 and Table 1. The volume fraction of each type of nanoparticle is 0.15.

ure S7). The lamellae first buckle, then break and dissolve into the disordered state, but later evolve into the parallel alignment. The curves in Figure 6 indicate that the nanocomposite with Janus nanoparticle possesses the fastest orientation dynamics in this shear field. From Supporting Information Figure S7, we can observe that Janus nanoparticles are kept anchoring in the interface between two phases during the shear process. These anchoring Janus nanoparticles can hold some old interface patches which can serve as the nuclei of interface formation, facilitating the formation of new interface through domain growth surrounding the nuclei as well as rotating or merging these old interface patches along the shear field.

The inset of Figure 6 demonstrates the shear viscosities of these systems at the later stage. Here we only compare the shear viscosity at the later time because the shear viscosity at the initial and middle stages is very sensitive to the original orientation structure. Clearly, the shear viscosity of the nanocomposite with Janus spheres is higher than those of the pure block copolymers and the block copolymer−homogeneous sphere composite. A previous study for the polymer−nanoparticle composite reveals that the attractive interaction between nanoparticles and polymer chains generates a higher viscosity than the pure polymers while the repulsion interaction between these both components leads to the lower viscosity than the pure polymers.[48] The Janus nanoparticles anchoring at the interface can attract both blocks of block copolymers, therefore increasing the viscosity of the nanocomposite. However the homogeneous nanoparticles only attract one block but simultaneously repulse the other block which decreases the viscosity of the composite. The above analysis demonstrates that the presence of Janus nanoparticles can accelerate the shear dynamics and enhance the shear viscosity of nanocomposites. These effects due to the Janus nanoparticles can be tuned by changing their architectures which consequently provides us a unique approach to create polymer nanocomposites with tunable and enhanced processing properties.

CONCLUSIONS

In summary, our simulations predict that the self-assembly of Janus nanoparticles at the interface of block copolymers is a viable approach to fabricate novel structures or superstructures on the nanometer scale. On the basis of this approach, oriented structures or superstructures on a macroscopic scale can be reached by using external fields to control the scaffold of block copolymers, which however is very difficult to realize from the self-assembly of particles in solutions. The results give a direct view of the deformation of polymer chains induced by Janus nanoparticles with various architectures, which is found to dominate the interfacial stabilization and kinetic pathway for structural evolution of the nanocomposites. We also evaluate the mechanism for the self-assembly of Janus nanoparticles confined within the block copolymer lamellae. Another important outcome of this study is that we show for the first time that the presence of Janus nanoparticles in block copolymers can provide us a unique approach to create polymer nanocomposites with tunable and enhanced processing properties. A potential conception implied in this study is the associated self-assembly between two or more amphiphilic building blocks. The coassembly of these amphiphilic building blocks may lead to diverse structures for new materials. This conception might also offer a unique view to understand some precise and complex self-assemblies in nature.

METHODS

We use the dissipative particle dynamics (DPD) technique which is a coarse-grained molecular dynamics (MD) approach and can capture the hydrodynamics of complex fluids.[49] For the complicated problem considered here DPD offers an approach that can be used for modeling physical phenomena occurring at larger time and spatial scales than typical MD as it utilizes a momentum-conserving thermostat and soft repulsive interactions between the beads representing clusters of molecules. In the present simulations, a bead i at position $\mathbf{r}_i$ surrounded by beads $j \neq i$ at $\mathbf{r}_j$ (distance vector $\mathbf{r}_{ij} = \mathbf{r}_i - \mathbf{r}_j$ and unit vector $e_{ij} = \mathbf{r}_{ij}/r_{ij}$ with $r_{ij} = |\mathbf{r}_{ij}|$) experiences a force with the components of conservative interaction force F^C, dissipative force F^D, random force F^R, and bond force F^S, that is, $f_i = \sum_{j\neq i}(F^C_{ij} + F^D_{ij} + F^R_{ij} + F^S_{ij})$ where the sum runs over all beads j.[49] The conservative force is given by $F^C_{ij} = \alpha_{ij}\omega^C(r_{ij})e_{ij}$, where α_{ij} is the maximum repulsion between beads i and j. For the interactions between like species, the repulsion parameter α_{ii} in F^C is chosen to be 25, and $\alpha_{AB} = 44.62$, $\alpha_{pq} = 25$, $\alpha_{Ap} = \alpha_{Bq} = 44.62$, $\alpha_{Aq} = \alpha_{Bp} = 18$ are set for the other interactions where A,B indicate the beads of two blocks in the diblock copolymers and p,q indicate the beads of two compartments of the Janus nanoparticles.[49,50] Clearly, the A and B blocks have strong affinities to the q and p sites of Janus nanoparticles, respectively. The weight function $\omega^C(r_{ij})$ is chosen as

$\omega^C(r_{ij}) = 1 - r_{ij}/r_c$ for $r_{ij} < r_c$ and $\omega^C(r_{ij}) = 0$ for $r_{ij} \geq r_c$, where r_c is the truncate distance. The random force F_{ij}^R and the dissipative force F_{ij}^D are given by $F_{ij}^R = \sigma\omega(r_{ij})\xi_{ij}\Delta t^{-1/2}e_{ij}$ and $F_{ij}^D = -^1/_2\sigma^2\omega(r_{ij})(v_{ij} \cdot e_{ij})e_{ij}$, where $v_{ij} = v_i - v_j$ and v_i denotes the velocity of bead i.[49] ξ_{ij} is a random number which has zero mean and unit variance. The noise amplitude, σ, is fixed at $\sigma = 3$ in the present simulations. The bonds between beads in the polymer chain are represented by $F_{ij}^S = C\mathbf{r}_{ij}$ with a stiffness constant $C = -4$.[49]

Here we use a modified velocity−Verlet algorithm due to Groot and Warren to solve the motion equation.[49] The radius of interaction, bead mass, and temperature are set as the unit, that is, $r_c = m = k_BT = 1$. A characteristic time scale is then defined as $\tau = (mr_c^2/k_BT)^{1/2}$. Our simulation box is $(30r_c)^3$ in size and with periodic boundary condition in all directions, which is large enough to avoid the finite size effects. A bead number density of $3/r_c^3$ is used. The time step of $\Delta t = 0.05\tau$ is chosen ensuring the accurate temperature control for the simulation system.[51]

Acknowledgment. We thank Heiko Schoberth for valuable discussions. L.-T.Y. acknowledges the hospitality of the University of Bayreuth. The financial support from Alexander von Humboldt Foundation and the VolkswagenStiftung is highly appreciated.

Supporting Information Available: Additional simulation results and video. This material is available free of charge *via* the Internet at http://pubs.acs.org.

REFERENCES AND NOTES

1. Alivisatos, A. P. Semiconductor Clusters, Nanocrystals, and Quantum Dots. *Science* **1996**, *271*, 933–937.
2. Frank, S.; Poncharal, P.; Wang, Z. L.; der Heer, W. A. Carbon Nanotube Quantum Resistors. *Science* **1998**, *280*, 1744–1746.
3. Sun, S. H.; Murray, C. B.; Weller, D.; Folks, L.; Moser, A. Monodisperse FePt Nanoparticles and Ferromagnetic FePt Nanocrystal Superlattices. *Science* **2000**, *287*, 1989–1992.
4. Huynh, W.; Dittmer, J. J.; Alivisatos, A. P. Hybrid Nanorod−Polymer Solar Cells. *Science* **2002**, *295*, 2425–2427.
5. Verma, A.; Uzun, O.; Hu, Y.; Hu, Y.; Han, H. S.; Watson, N.; Chen, S.; Irvine, D. J.; Stellacci, F. Surface-Structure-Regulated Cell-Membrane Penetration by Monolayer-Protected Nanoparticles. *Nat. Mater.* **2008**, *7*, 588–595.
6. Zhang, Z; Glotzer, S. C. Self-Assembly of Patchy Particles. *Nano Lett.* **2004**, *4*, 1407–1413.
7. Bianchi, E.; Largo, J.; Tartaglia, P.; Zccareli, E.; Sciortino, F. Phase Diagram of Patchy Colloids: Towards Empty Liquids. *Phys. Rev. Lett.* **2006**, *97*, 168301.
8. Kern, N.; Frenkel, D. Fluid−Fluid Coexistence in Colloidal Systems with Short-Ranged Strongly Directional Attraction. *J. Chem. Phys.* **2003**, *118*, 9882–9889.
9. Srinivas, G.; Pitera, J. W. Soft Patchy Nanoparticles from Solution-Phase Self-Assembly of Binary Diblock Copolymers. *Nano Lett.* **2008**, *8*, 611–618.
10. Glotzer, S. C. Some Assembly Required. *Science* **2004**, *306*, 419–420.
11. Glotzer, S. C.; Solomon, M. J. Anisotropy of Building Blocks and Their Assembly into Complex Structures. *Nat. Mater.* **2007**, *6*, 557–562.
12. Fejer, S. N.; Wales, D. J. Helix Self-Assembly from Anisotropic Molecules. *Phys. Rev. Lett.* **2007**, *99*, 086106.
13. Tang, Z. Y.; Zhang, Z. L.; Wang, Y.; Glotzer, S. C.; Kotov, N. A. Self-Assembly of CdTe Nanocrystals into Free-Floating Sheets. *Science* **2006**, *314*, 274–278.
14. de Gennes, P. G. Soft Matter. *Rev. Mod. Phys.* **1992**, *64*, 645–648.
15. Walther, A.; Müller, A. H. E. Janus Particles. *Soft Matter* **2008**, *4*, 663–668.
16. Roh, K. H.; Martin, D. C.; Lahann, J. Biphasic Janus Nanoparticles with Nanoscale Anisotropy. *Nat. Mater.* **2005**, *4*, 759–762.
17. Jiang, S.; Granick, S. Controlling the Geometry (Janus Balance) of Amphiphilic Colloidal Particles. *Langmuir* **2008**, *24*, 2438–2445.
18. Erhardt, R.; Zhang, M.; Böker, A.; Zettl, H.; Abetz, C.; Frederik, P.; Krausch, G.; Abetz, V.; Müller, A. H. E. Amphiphilic Janus Micelles with Polystyrene and Poly(methacrylic acid) Hemispheres. *J. Am. Chem. Soc.* **2003**, *125*, 3260–3267.
19. Wang, C.; Xu, C.; Zeng, J.; Sun, S. Recent Progress in Syntheses and Applications of Dumbbell-like Nanoparticles. *Adv. Mater.* **2009**, *21*, 3045–3052.
20. Nie, L.; Liu, S. Y.; Shen, W. M.; Chen, D. Y.; Jiang, M. One-Pot Synthesis of Amphiphilic Polymeric Janus Particles and Their Self-Assembly into Supermicelles with a Narrow Size Distribution. *Angew. Chem., Int. Ed.* **2007**, *46*, 6321–6324.
21. Hong, L.; Cacciuto, A.; Luijten, E.; Granick, S. Cluster of Charged Janus Spheres. *Nano Lett.* **2006**, *6*, 2510–2514.
22. van Blaaderen, A. Materials Science: Colloids Get Complex. *Nature* **2006**, *439*, 545–546.
23. van Workum, K.; Douglas, J. F. Symmetry, Equivalence, and Molecular Self-Assembly. *Phys. Rev. E* **2006**, *73*, 031502.
24. Tefort, A.; Bowden, N.; Whitesides, G. M. Three-Dimensional Self-Assembly of Millimetre-Scale Components. *Nature* **1997**, *386*, 162–164.
25. Onoe, H.; Matsumoto, K.; Shimoyama, I. Three-Dimensional Sequential Self-Assembly of Microscale Objects. *Small* **2007**, *3*, 1383–1389.
26. Zhang, X.; Zhu, Y.; Granick, S. Hydrophobicity at a Janus Interface. *Science* **2002**, *295*, 663–666.
27. Glaser, N.; Adams, D. J.; Böker, A.; Krausch, G. Janus Particles at Liquid−Liquid Interfaces. *Langmuir* **2006**, *22*, 5227–5229.
28. Walther, A.; Matussek, K.; Müller, A. H. E. Engineering Nanostructured Polymer Blends with Controlled Nanoparticle Location Using Janus Nanoparticles. *ACS Nano* **2008**, *2*, 1167–1178.
29. Stratford, K.; Adhikari, R.; Pagonabarraga, I.; Desplat, J. C.; Cates, M. E. Colloidal Jamming at Interfaces: A Route to Fluid-Biocontinous Gels. *Science* **2005**, *309*, 2198–2201.
30. Chung, H. J.; Ohno, K.; Fukuda, T.; Composto, R. J. Self-Regulated Structures in Nanocomposites by Directed Nanoparticle Assembly. *Nano Lett.* **2005**, *5*, 1878–1882.
31. Lin, Y.; Böker, A.; He, J.; Sill, K.; Xiang, H.; Abetz, C.; Li, X.; Emrick, T.; Long, S.; Wang, Q.; *et al*. Self-Directed Self-Assembly of Nanoparticle/Copolymer Mixtures. *Nature* **2005**, *434*, 55–59.
32. Lopes, W. A.; Jaeger, H. M. Hierarchical Self-Assembly of Metal Nanostructures on Diblcok Copolymer Scaffolds. *Nature* **2001**, *414*, 735–738.
33. Deshmukh, R. D.; Liu, Y.; Composto, R. J. Two-Dimensional Confinement of Nanorods in Block Copolymer Domains. *Nano Lett.* **2007**, *7*, 3662.
34. Chiu, J. J.; Kim, B. J.; Kramer, E. J.; Pine, D. J. Control of Nanoparticle Location in Block Copolymers. *J. Am. Chem. Soc.* **2005**, *127*, 5036–5037.
35. Kim, J. U.; Matsen, M. W. Positioning Janus Nanoparticles in Block Copolymer Scaffolds. *Phys. Rev. Lett.* **2009**, *102*, 078303.
36. Thompson, R. B.; Ginzburg, V. V.; Matsen, M.W.; Balazs, A. C. Predicting the Mesophases of Copolymer−Nanoparticle Composite. *Science* **2001**, *292*, 2469–2472.
37. Bockstaller, M. R.; Lapetnikov, Y.; Margel, S.; Thomas, E. L. Size-Selective Organization of Enthalpic Compatibilized Nanocrystals in Ternary Block Copolymer/Particle Mixtures. *J. Am. Chem. Soc.* **2003**, *125*, 5276–5277.
38. Alexeev, A.; Uspal, W. E.; Balazs, A. C. Harnessing Janus Nanoparticles to Create Controllable Pores in Membranes. *ACS Nano* **2008**, *2*, 1117–1122.
39. Hore, M. J.; Laradji, M. Prospects of Nanorods as an Emulsifying Agent of Immiscible Blends. *J. Chem. Phys.* **2008**, *128*, 054901.
40. Thurn-Albrecht, T.; Schotter, J.; Kastle, C. A.; Emley, N.; Shibauchi, T.; Krusin-Elbaum, L.; Guarini, K.; Black, C. T.; Tuominen, M. T.; Russell, T. P. Ultrahigh-Density Nanowire Arrays Grown in Self-Assembled Diblock Copolymer Templates. *Science* **2000**, *290*, 2126–2129.

41. Chen, Z. R.; Kornfield, J. A.; Smith, S. D.; Grothaus, J. T.; Satkowski, M. M. Pathways to Macroscale Order in Nanostructured Block Copolymers. *Science* **1997**, *277*, 1248–1253.
42. Pryamitsyn, V.; Ganesan, V. Strong Segregation Theory of Block Copolymer−Nanoparticle Composites. *Macromolecules* **2006**, *39*, 8499–8510.
43. Nonomura, Y.; Komura, S.; Tsujii, K. Adsorption of Disk-Shaped Janus Beads at Liquid−Liquid Interfaces. *Langmuir* **2004**, *20*, 11821–11823.
44. Helfand, E.; Tagami, Y. Theory of the Interface between Immiscible Polymers II. *J. Chem. Phys.* **1972**, *56*, 3592–3601.
45. de Gennes, P. G.; Prost, J. *The Physics of Liquid Crystals*; Clarendon Press: Oxford, 1993.
46. Lees, A. W.; Edwards, S. F. The Computer Study of Transport Processes under Extreme Conditions. *J. Phys. (Paris)* **1972**, *C5*, 1921.
47. Allen, M. P.; Tildesley, D. J. *Computer Simulation of Liquids*; Clarendon Press: Oxford, 1987.
48. Smith, G. D.; Bedrov, D.; Li, L.; Byutner, O. A Molecular Dynamics Simulation Study of the Viscoelastic Properties of Polymer Nanocomposites. *J. Chem. Phys.* **2002**, *117*, 9478–9489.
49. Groot, R. D.; Warren, P. B. Dissipative Particle Dynamics: Bridging the Gap between Atomistic and Mesoscopic Simulation. *J. Chem. Phys.* **1997**, *107*, 4423–4435.
50. Yan, L. T.; Yu, X. Enhanced Permeability of Charged Dendrimers across Tense Lipid Bilayer Membranes. *ACS Nano* **2009**, *3*, 2171–2176.
51. Vattulainen, I.; Karttunen, M.; Besold, G.; Polson, J. M. Integration Schemes for Dissipative Particle Dynamics Simulations: From Softly Interacting Systems towards Hybrid Models. *J. Chem. Phys.* **2002**, *116*, 3967–3979.